

Article

Influence of Scale Effect on Strength and Deformation Characteristics of Rockfill Materials

Hongxing Han ^{1,*} , Jing Li ², Jicun Shi ^{1,*} and Cuina Yang ¹¹ School of Civil Engineering and Architecture, Xinxiang University, Xinxiang 453003, China² Architectural Teaching and Research Group, Xinxiang University of Broadcast & Television, Xinxiang 453000, China

* Correspondence: hxhan@whu.edu.cn (H.H.); jicun.shi070@xxu.edu.cn (J.S.)

Abstract: The hybrid method was adopted to model the original gradation of rockfill materials. According to the specification requirements, three simulated gradations of rockfill materials have been obtained. By the same token, the corresponding maximum particle sizes are 20 mm, 40 mm and 60 mm, respectively. With samples prepared under the same criterion of relative density, the scale effect on strength and deformation characteristics of the rockfill materials were studied by large-scale and consolidated-drained triaxial compression tests. The results show that when the confining pressure is higher, the peak deviator stress decreases with the increase of the maximum particle size. With the increase of the maximum particle size, the cohesion of rockfill materials gradually increases and the internal friction angle gradually decreases. Under the condition of the same maximum particle size, with the increase of confining pressure, the volume strain at the phase transition increases gradually, while the stress ratio at the phase transition decreases. Under the same confining pressure, the larger the particle size is, the smaller the volume strain becomes and the lower the stress ratio at the phase transition is. Therefore, the research results can provide a theoretical basis for establishing the constitutive model of rockfill materials considering the scale effect.

Keywords: rockfill materials; scale effect; triaxial test; maximum particle size; confining pressure; deformation characteristics



Citation: Han, H.; Li, J.; Shi, J.; Yang, C. Influence of Scale Effect on Strength and Deformation Characteristics of Rockfill Materials. *Materials* **2022**, *15*, 5467. <https://doi.org/10.3390/ma15155467>

Academic Editor: Lukasz Sadowski

Received: 23 June 2022

Accepted: 2 August 2022

Published: 8 August 2022

Publisher's Note: MDPI stays neutral with regard to jurisdictional claims in published maps and institutional affiliations.



Copyright: © 2022 by the authors. Licensee MDPI, Basel, Switzerland. This article is an open access article distributed under the terms and conditions of the Creative Commons Attribution (CC BY) license (<https://creativecommons.org/licenses/by/4.0/>).

1. Introduction

As the main filling material of earth rock dams, rockfill materials are widely used because they can be adapt to more complex geological conditions [1–3]. Block stone, crushed stone, stone slag, sandy soil, stone chips, backfill, and mixed soil containing a large number of coarse particles in cohesive soil are materials often used in engineering [4–10]. At present, with the continuous increase in the height of earth rock dams, the particle size of rockfill materials is also larger, some of which reach 600~800 mm, and some even reach 1000 mm [10,11]. Under the indoor triaxial test condition [2], the maximum particle size of the sample shall not exceed 1/5 of the sample diameter D. Limited by the size of the test instrument. The rockfill materials that exceed the maximum allowable particle size for the test must be reduced. There are great differences in the macro mechanical properties of rockfill materials replaced by scales of different sizes [3,10–13], which is the scale effect. In recent years, the research on scaling effect mainly focuses on two aspects [2]: on the one hand, it is to increase the sample size and restore the in situ size of rockfill as much as possible to reduce the impact of scaling [1,12,14]. On the other hand, it is to carry out research on the law of scaling effect, hoping to use the results of large- and medium-sized tests to deduce the mechanical properties of the original grade rockfill materials. Results of triaxial tests on rockfill materials by Rahmani and Panah [15] revealed that particle breakage increased with the increase maximum particle sizes of soft rockfill materials, and proposed a calculation method of relative crushing rate [2]. Another important factor for rockfill materials breakage is the critical state behavior of constituting rockfill aggregates [16].

In these studies, the fractal dimension proposed by Han [17] was used to evaluate the relationship between particle distribution and its mechanical properties. However, the maximum particle size of the sample is closely related to its mechanical properties [18]. The distribution of the particle size of rockfill has a great impact on its strength and deformation characteristics. Yang et al. [19] used a large triaxial apparatus to conduct triaxial tests on rockfill. The study found that the volume strain of the aggregate decreased with the increase of the maximum particle size, and the peak deviator stress increased with the increase of the maximum particle size. The parallel gradation and combination methods [20] are widely acknowledged in testing and designing of rockfill, inevitably instigating the use of reduced maximum particle size. Ventini et al. [21] studied the influence of gradation on the deformation characteristics of rockfill and believed that the volumetric strain of the two rockfill materials under low stress was similar to that of saturated soil samples. The research shows that the mechanical properties of the reduced alternative material are quite different from those of the original granular material [15–21], but the current understanding is not enough to quantitatively evaluate its impact, so it is necessary to conduct in-depth discussion.

In view of this, this paper has been used the hybrid method to reduce the original gradation into three simulated gradations according to the specification, and the corresponding maximum particle sizes are 20 mm, 40 mm and 60 mm, respectively. The same relative density is used as the sample preparation standard, and the ylsz30-3 large-scale dynamic and static triaxial apparatus is used to conduct isobaric consolidation drainage shear tests under different confining pressures on three simulated gradations. The test results are analyzed to study the influence of scaling effect on the strength and deformation characteristics of rockfill.

2. Experimental Details

2.1. Experimental Equipment

A YLSZ30-3 large dynamic and static triaxial testing machine was used in this test. Sample size is $\phi 300$ mm \times 600 mm, as shown in Figure 1. The equipment is used to study the strength and deformation characteristics of dam materials under different stress paths. The main technical parameters are: maximum axial load 2500 kN, maximum axial vertical deformation 300 mm, maximum confining pressure 6.0 MPa, and shear speed 0.2–2 mm/min. Strain control is adopted in the test, and the ratio of the maximum allowable particle size of the sample to the diameter of the sample is $d_{\max}/D = 0.2$.

2.2. Experimental Materials

The rockfill materials studied in this paper were selected from the main rockfill material of a rockfill dam. The lithology was weathered granite and the rock block was hard. The maximum particle size is 200 mm, the particle proportion is 2.76, the nonuniformity coefficient is $C_u = 11.68$, and the curvature coefficient is $C_c = 1.31$. Using mixed method to reduce the prototype grading of rockfill. The number is HH. The maximum particle size of the simulated gradation is 60, 40 and 20 mm, respectively, which is used as the subscript of the number to distinguish. For example, HH₂₋₆₀ represents the reduction multiple $n = 2$, and the maximum particle size after the reduction is 60 mm. Figure 2 shows grain-size distribution curves of rockfill materials. The simulated grading and results of rockfill materials are shown in Table 1.

The sample is prepared by layered vibration method, 3 layers, each layer of 20 cm, compacted to the design height by surface oscillator, and the frequency is set to 50 Hz. The prepared samples are saturated by filling water at the bottom and pumping air at the top. After consolidation, they are sheared at a strain rate of 1 mm/min. There are three groups of confining pressure tests. The test control conditions are shown in Table 2. The test termination condition is that the axial strain of the specimen is 15%. Typical photographs of the sample before and after the test are shown in Figure 3.

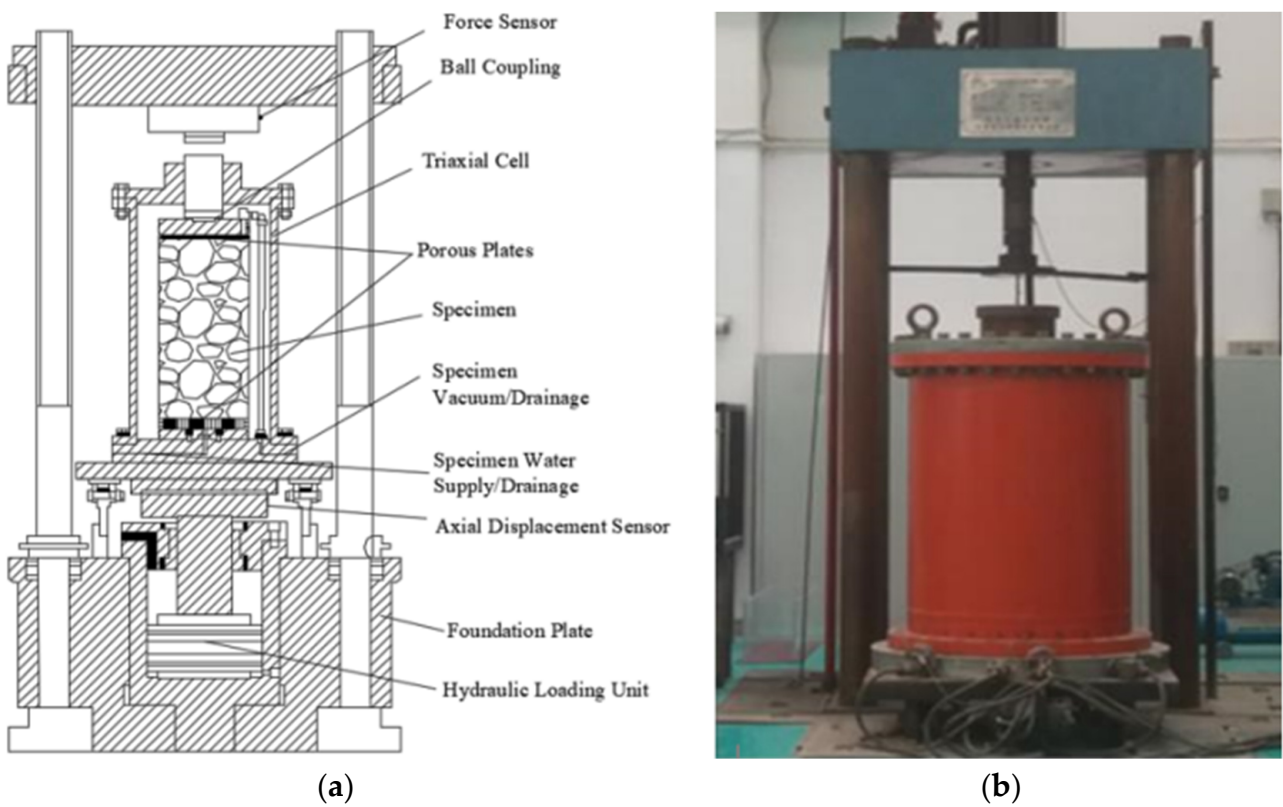


Figure 1. Large-scale triaxial compression apparatus: (a) overall view of the apparatus; and (b) pressure stabilization techniques.

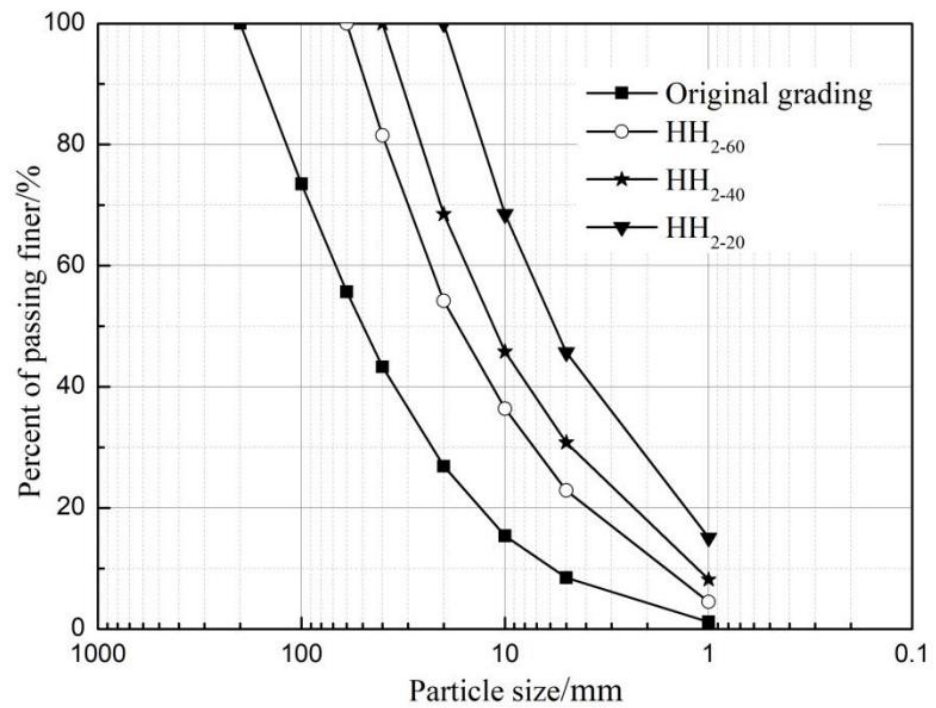


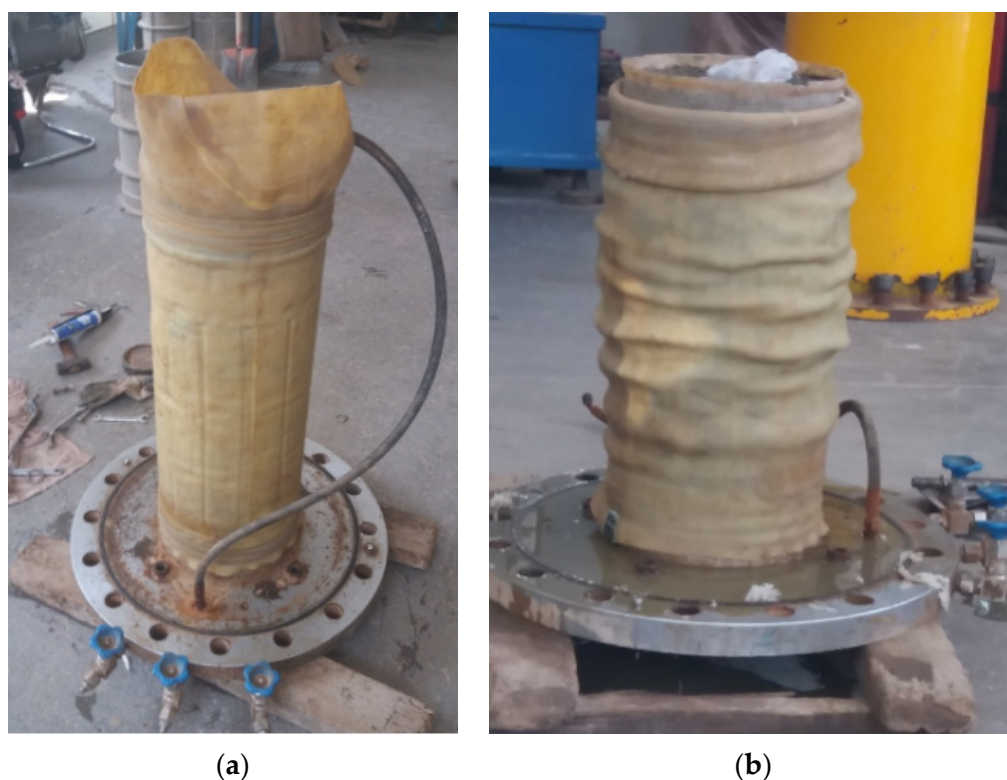
Figure 2. Grain-size distribution curves of rockfill materials.

Table 1. The test gradation of rockfill materials and tested results.

Hybrid Method	Effective Particle Size d_{10}	Intermediate Particle Size d_{30}	Controlled Particle Size d_{60}	Nonuniformity Coefficient C_u	Curvature Coefficient C_c
HH ₂₋₆₀	2.89	9.86	24.55	8.49	1.37
HH ₂₋₄₀	2.89	8.41	18.68	6.46	1.31
HH ₂₋₂₀	2.89	6.69	11.47	3.97	1.35

Table 2. The test plan.

Hybrid Method	Sample Diameter/mm	$d_{max}/(mm)$	$\rho_d/(G \cdot cm^{-3})$	$\sigma_3/(KPa)$
HH ₂₋₆₀	300	60	2.181	600, 900, 1200
HH ₂₋₄₀	300	40	2.155	600, 900, 1200
HH ₂₋₂₀	300	20	2.114	600, 900, 1200

**Figure 3.** Typical photographs of the sample before and after the test ($\sigma_3 = 600$ kPa). (a) Loading sample. (b) Failure specimen.

3. Results and Discussion

3.1. Strength Characteristic Analysis

Three groups of rockfill materials are obtained by the hybrid scale method. The relationship curve between peak deviator stress $(\sigma_1 - \sigma_3)_f$ and confining pressure σ_3 of each group samples under different confining pressures is shown in Figure 4. It can be seen from Figure 4 that under the same confining pressure, the peak deviator stress of HH₂₋₂₀ material is the largest and that of HH₂₋₆₀ material is the smallest; under the same maximum particle size, the peak intensity increases with the improvement of confining pressure, which is approximately linear.

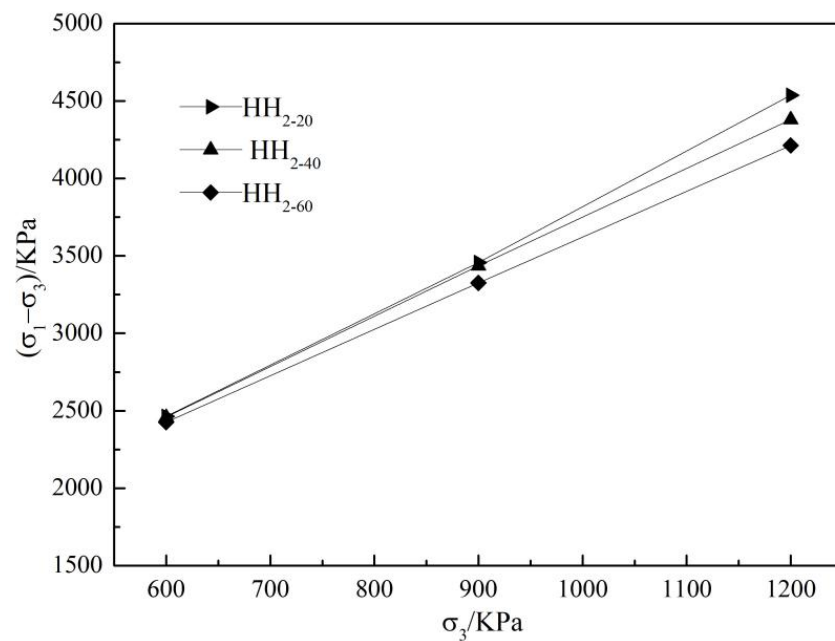


Figure 4. The relationship between peak strength and confining pressure.

Rockfill materials are cohesionless soil, but gravel, pebble and rockfill are closely meshed with each other under dense conditions, and there is a “biting force”, which is similar to the cohesion of cohesive soil in macro. Table 3 lists the strength index of different size values. It can be seen from Table 3 that the cohesion increases with the increase of the maximum particle size of rockfill materials, while the internal friction angle decreases with the increase of the maximum particle size.

Table 3. Strength index of different size value.

Hybrid Method	σ_3/kPa	$(\sigma_1 - \sigma_3)/\text{kPa}$	c/kPa	$\varphi/(\text{°})$
HH ₂₋₂₀	600	2463.2	125.37	38.33
	900	3456.3		
	1200	4535.8		
HH ₂₋₄₀	600	2459.4	148.01	37.69
	900	3435.1		
	1200	4379.2		
HH ₂₋₆₀	600	2426.3	166.87	36.74
	900	3325.5		
	1200	4212.7		

The edges and corners of particles with larger particle size are relatively sharp. The more prone it is to stress concentration, the more likely the particles are to be broken. After failure, the particle size stress is redistributed, and the particle size connection stress becomes weak, so the internal friction angle of rockfill materials increases.

3.2. Analysis of Deformation Characteristics

The content of coarse material is more after that the coarse material is reduced by mixing method and induced large shrinkage deformation [22]. In order to further study the influence of the maximum particle size d_{max} of rockfill materials on its dilatancy, this paper supplies the relationship between the volume strain value ε_{v0} and the confining pressure σ_3 of the rockfill specimen at the phase change position (the turning point of volume from compression to expansion) under different confining pressures of three groups after scale reduction, as shown in Figure 5. It can be seen from Figure 5 that the volume strain values ε_{v0} at the phase transformation of three groups of samples increase with the increase of

confining pressure σ_3 . Under the same confining pressure, the volume strain ε_{v0} obtained by HH₂₋₆₀ scale method is at the bottom side, however that obtained by HH₂₋₂₀ scale method is at the top side, and that obtained by HH₂₋₄₀ scale method is between the HH₂₋₂₀ and HH₂₋₆₀. The larger the maximum particle size d_{max} is, the larger the volume strain ε_{v0} is.

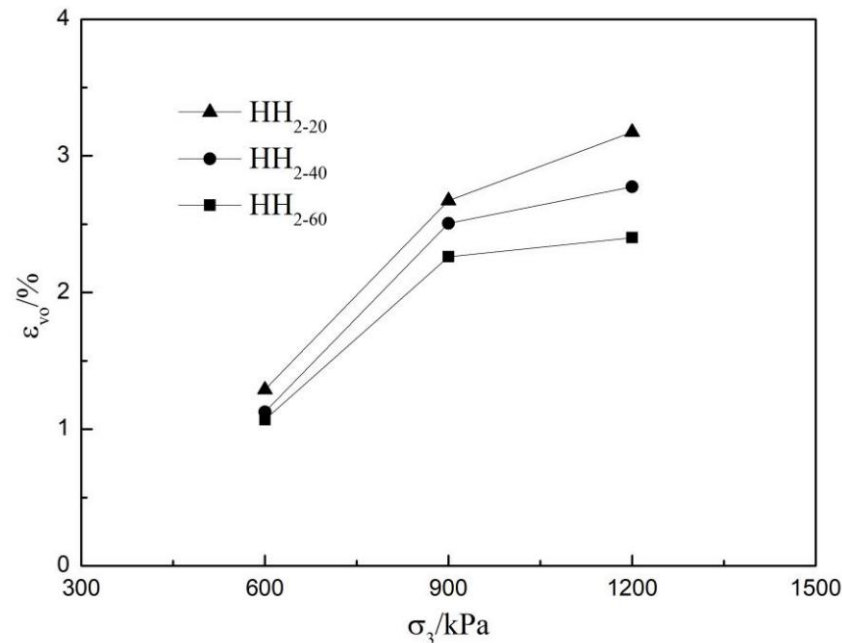


Figure 5. Relationship between volume strain ε_{v0} and confining pressure σ_3 at phase change.

The accurate description of dilatancy is very important for the constitutive model of dilatancy. When some shear expansion models are established, the stress ratio at the transformation (M_0 , $M_0 = q_0 / p'_0$, where q_0 is the generalized shear stress at the transformation, p'_0 is the average principal stress at the transformation) is often used to express the shear expansion equation or hardening parameters. Three groups of test data are sorted out, and the relationship between M_0 and σ_3 /kPa is drawn, as shown in Figure 6. From Figure 6, it can be seen that the stress ratio M_0 of rockfill samples at the transformation point decreases with the increase of confining pressure σ_3 after three groups of downscales, and a good linear relationship is formed with the confining pressure. The following formula can be used for fitting:

$$M_0 = a \times \frac{\sigma_3}{\text{kPa}} + b \quad (1)$$

where: a , b are test parameters, see Figure 6 for specific values.

3.3. Nonlinearity of Shear Strength

The shear strength of soil is the resistance of soil to the shear stress produced by external load. In 1776, based on a large number of experiments, the famous Coulomb formula was proposed [23].

$$\tau_f = c + \sigma_n \tan \varphi \quad (2)$$

where: τ_f is shear strength of damaged surface, σ_n is normal stress of damaged surface; c is cohesive force, φ is internal friction angle.

Duncan has developed the hyperbolic stress–strain model on the basis of Coulomb [24], and adopted the logarithmic form for the strength envelope of cohesionless soil bending, the expression is as follows.

$$\varphi = \varphi_0 - \Delta\varphi \lg\left(\frac{\sigma_3}{P_a}\right) \quad (3)$$

where: σ_3 is the small main stress, p_a is the atmospheric pressure, φ_0 , $\Delta\varphi$ is the material parameter.

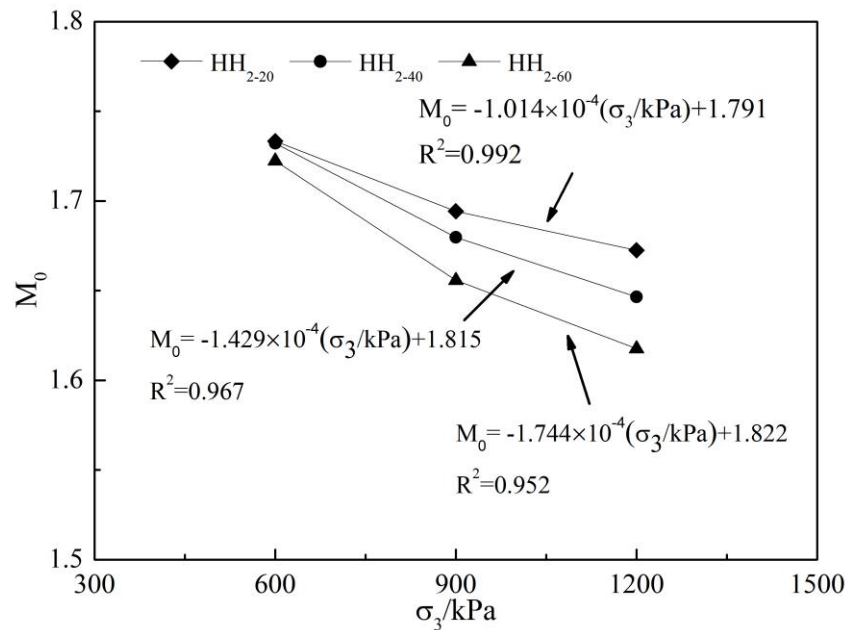


Figure 6. Relationship between stress ratio M_0 and confining pressure σ_3 at phase change.

Figure 7 shows the relationship between nonlinear strength index φ_0 , $\Delta\varphi$ and d_{\max} . It can be seen from Figure 7 that the nonlinear strength index φ_0 and $\Delta\varphi$ both increases with the increase of the maximum particle size d_{\max} . Among them, the value φ_0 and $\Delta\varphi$ of HH₂₋₄₀ increases by 1.449° and 1.818° compared with the corresponding value of HH₂₋₂₀, while the value of HH₂₋₆₀ increases by 0.885° and 1.470° compared with the corresponding value of HH₂₋₄₀. When the particles are larger, the biting force between soil particles is better, and the correlation with d_{\max} is weaker.

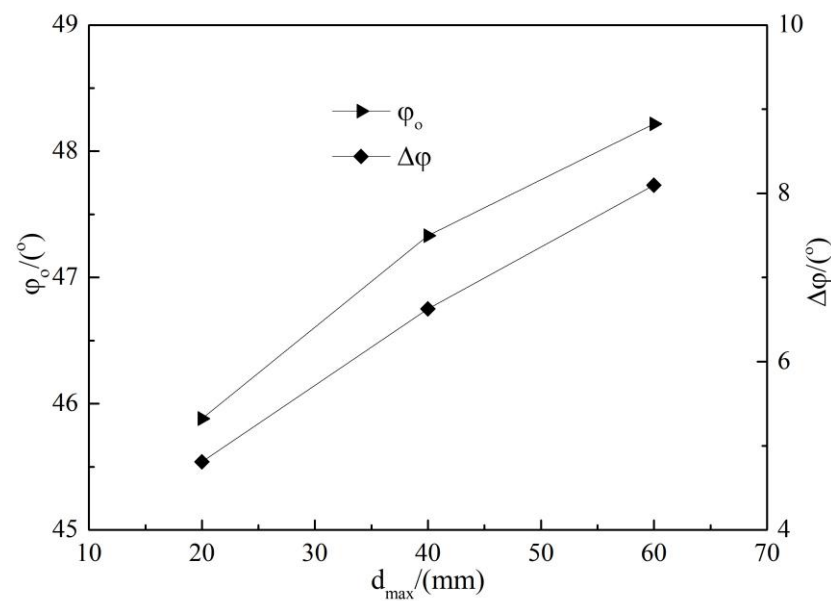


Figure 7. Relationship between φ_0 , $\Delta\varphi$ and d_{\max} .

4. Conclusions

- (1) Under the same confining pressure, the smaller the maximum particle size d_{\max} is in the three groups of granular materials, the larger the corresponding peak deviator

- stress $(\sigma_1 - \sigma_3)_f$, the volume strain ε_{vo} and stress ratio M_0 are at the phase transformation, which indicates that the soil particles have a higher overturning capacity, and the macroscopic performance is that HH₂₋₂₀ material has a stronger dilatancy.
- (2) With the increase of confining pressure σ_3 , the peak deviator stress $(\sigma_1 - \sigma_3)_f$ and volume strain ε_{vo} in the three groups of granular materials gradually increased, while the stress ratio M_0 at the phase transformation gradually decreased, and the stress ratio M_0 at the phase transformation showed a good linear relationship with the confining pressure σ_3 .
 - (3) In the linear shear strength index, with the increase of the maximum particle size d_{max} , the cohesion of rockfill materials c gradually increases, while the internal friction angle φ of rockfill materials shows a downward trend. Among the nonlinear shear strength indexes, the strength indexes φ_0 and $\Delta\varphi$ in the three groups of granular materials increase with the increase of the maximum particle size d_{max} .

Author Contributions: Conceptualization, H.H. and J.L.; data curation, J.S. and C.Y.; writing—review, C.Y.; supervision, H.H. and J.S. All authors have read and agreed to the published version of the manuscript.

Funding: This work was supported by Xinxiang University Doctoral Research Starting Fund (1366020159), Science and technology guidance plan project of Henan Civil Architecture Society (202104) and Scientific research projects of higher learning institutions in Henan Province (21B140005).

Informed Consent Statement: Not applicable.

Data Availability Statement: All data used to support the findings of this study are available from the corresponding author upon request.

Conflicts of Interest: The authors declare no conflict of interest.

References

1. Khonji, A.; Bagherzadeh-Khalkhali, A.; Aghaei-Araei, A. Experimental investigation of rockfill particle breakage under large-scale triaxial tests using five different breakage factors. *Powder Technol.* **2020**, *363*, 473–487. [\[CrossRef\]](#)
2. Zhou, Y.F.; Wang, J.J.; Wang, A.G.; Yang, X. Experimental Study on Scale Effects of Particle Breakage of Rockfill Materials. *Water Resour. Power* **2021**, *39*, 165–168.
3. Xiao, Y.; Meng, M.; Daouadji, A.; Chen, Q.; Wu, Z.; Jiang, X. Effects of particle size on crushing and deformation behaviors of rockfill materials. *Geosci. Front.* **2020**, *11*, 375–388. [\[CrossRef\]](#)
4. Andjelkovic, V.; Pavlovic, N.; Lazarevic, Z.; Radovanovic, S. Modelling of shear strength of rockfills used for the construction of rockfill dams. *Soils Found.* **2018**, *58*, 881–893. [\[CrossRef\]](#)
5. Mazaheri, A.R.; Komasi, M.; Veisi, M.; Nasiri, M. Dynamic Analysis of Earth Dam using Numerical Method—A Case Study Doyraj Earth Dam. *Acta Geotech. Slov.* **2021**, *18*, 65–78. [\[CrossRef\]](#)
6. Mase, L.Z.; Likitlersuang, S.; Tobita, T. Cyclic behaviour and liquefaction resistance of Izumio sands in Osaka, Japan. *Mar. Georesources Geotechnol.* **2019**, *37*, 765–774. [\[CrossRef\]](#)
7. Sukkarak, R.; Tanapalungkorn, W.; Likitlersuang, S.; Ueda, K. Liquefaction analysis of sandy soil during strong earthquake in Northern Thailand. *Soils Found.* **2021**, *61*, 1302–1318. [\[CrossRef\]](#)
8. Kusumawardani, R.; Suryolelono, K.B.; Suhendro, B.; Rifai, A. The dynamic response of unsaturated clean sand at a very low frequency. *Int. J. Technol.* **2016**, *7*, 123–131. [\[CrossRef\]](#)
9. Ermolovich, E.A.; Ivannikov, A.L.; Khayrutdinov, M.M.; Kongar-Syuryun, C.B.; Tyulyaeva, Y.S. Creation of a Nanomodified Backfill Based on the Waste from Enrichment of Water-Soluble Ores. *Materials* **2022**, *15*, 3689. [\[CrossRef\]](#)
10. Han, H.; Ma, Y.; He, W.; Yang, W.; Fu, X. Numerical Simulation of Rockfill Materials Based on Fractal Theory. *Appl. Sci.* **2022**, *12*, 289. [\[CrossRef\]](#)
11. Wu, E.; Zhu, J.; Guo, W.; Zhang, Z. Effect of Gradation on the Compactability of Coarse-Grained Soils. *KSCE J. Civ. Eng.* **2020**, *24*, 356–364. [\[CrossRef\]](#)
12. Ovalle, C.; Linero, S.; Dano, C.; Bard, E.; Hicher, P.Y.; Osses, R. Data Compilation from Large Drained Compression Triaxial Tests on Coarse Crushable Rockfill Materials. *J. Geotech. Geoenviron. Eng.* **2020**, *146*, 06020013. [\[CrossRef\]](#)
13. Chakraborty, U.B.; Honkanadavar, N.P. Factors Influencing the Behavior of Rockfill Materials. *Adv. Geotech. Struct. Eng.* **2021**, *143*, 65–75.
14. Zhang, X.; Gao, Y.; Wang, Y.; Yu, Y.Z.; Sun, X. Experimental study on compaction-induced anisotropic mechanical property of rockfill material. *Front. Struct. Civ. Eng.* **2021**, *15*, 109–123. [\[CrossRef\]](#)

15. Rahmani, H.; Panah, A.K. Effect of particle size and saturation conditions on the breakage factor of weak rockfill materials under one-dimensional compression testing. *Geomech. Eng.* **2020**, *21*, 315–326.
16. Ning, F.; Liu, J.; Kong, X.; Zou, D. Critical State and Grading Evolution of Rockfill Material under Different Triaxial Compression Tests. *Int. J. Geomech.* **2020**, *20*, 04019154. [[CrossRef](#)]
17. Han, H.; Chen, W.; Huang, B.; Fu, X. Numerical simulation of the influence of particle shape on the mechanical properties of rockfill materials. *Eng. Comput.* **2017**, *34*, 2228–2241. [[CrossRef](#)]
18. Chakraborty, U.B.; Honkanadavar, N.P. Engineering Behavior of Alluvial Rockfill Material. *Ground Charact. Found.* **2021**, *167*, 261–266.
19. Yang, G.; Jiang, Y.; Nimbalkar, S.; Sun, Y.; Li, N. Influence of Particle Size Distribution on the Critical State of Rockfill. *Adv. Civ. Eng.* **2019**, *167*, 8963971. [[CrossRef](#)]
20. Wei, K.M.; Zhu, S.H.; Yu, X.H. Influence of the scale effect on the mechanical parameters of coarse-grained soils. *IJST-Trans-Actions Civ. Eng.* **2014**, *38*, 75–84.
21. Ventini, R.; Flora, A.; Lirer, S.; Mancuso, C. On the Effect of Grading and Degree of Saturation on Rockfill Volumetric Deformation. *Geotech. Res. Land Prot. Dev.* **2019**, *40*, 462–471.
22. Wang, H.L.; Huang, X.H.; Xie, B. Study on strength and deformation characteristics of coarse aggregate after different grading scale methods. *J. Hebei Univ. Eng. (Nat. Sci. Ed.)* **2019**, *36*, 36–40,74.
23. Kong, X.J.; Song, L.F.; Xu, B.; Zou, D.G. Correlation and distribution model for nonlinear strength parameters of rockfill based on Copula function. *Chin. J. Geotech. Eng.* **2020**, *42*, 797–807.
24. Duncan, J.M.; Byrne, P.; Wong, K.S.; Mabry, P. *Strength Stress-Strain and Bulk Modulus Parameters for Finite Element-Analysis of Stress and Movements in Soil Masses*; Report No. UCB/GT/80-01 Berkeley; Department of Engineering, University of California: Berkeley, CA, USA, 1980.